Electronic Supplementary Material (ESI) for Dalton Transactions.
This journal is © The Royal Society of Chemistry 2016

Supplemental Material

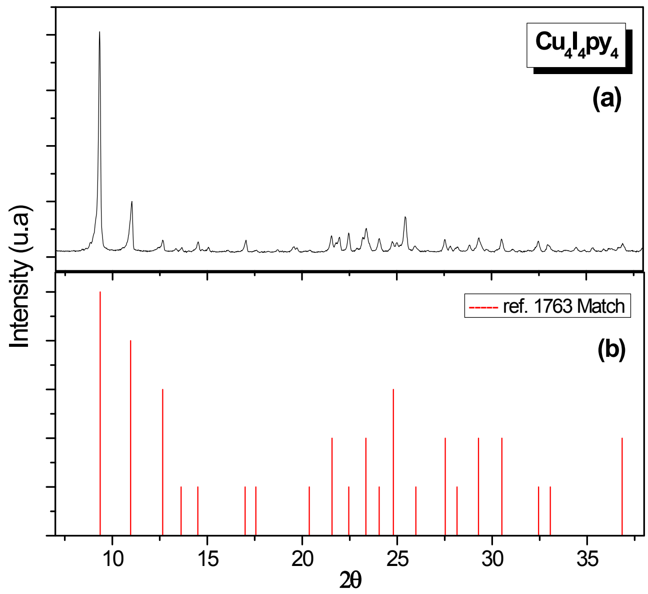

Figure S1. Diffractogram for the powder sample $Cu_4I_4py_4$ dried in N_2 flow. (a) $Cu_4I_4py_4$ powder (b): crystallographic record (Match) for the $Cu_4I_4py_4$.

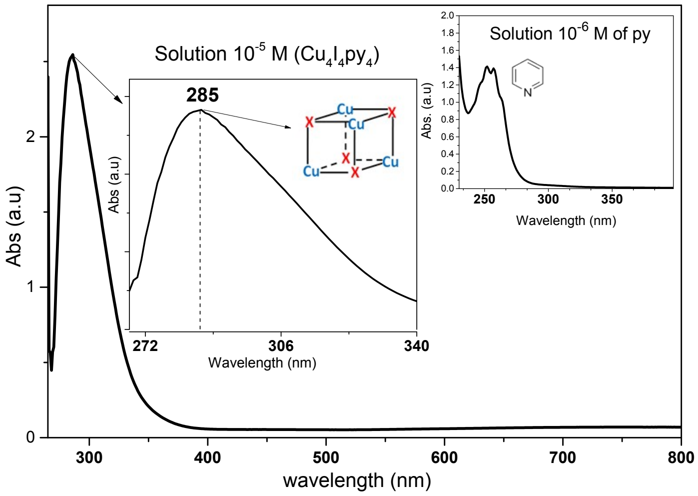

Figure S2. Absorption spectrum in the range of 200-800 nm for a solution 10_{-5} M of $Cu_4I_4py_4$ in CH_2Cl_2 after subtraction of ligand (py). Detail: Solution 10_{-6} M of pyridine in CH_2Cl_2.

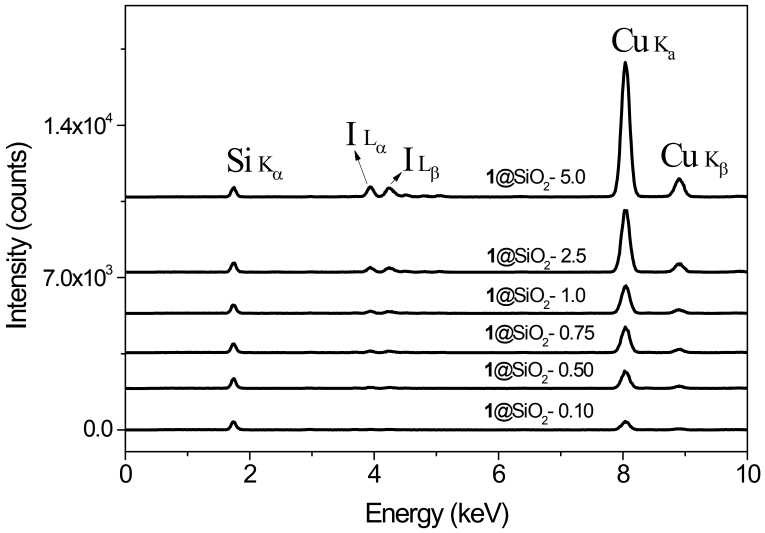

Figure S3. XRF spectra for the 1@SiO_2-z materials obtained from solutions with z = 0.10, 0.50, 0.75, 1.00, 2.50 and 5.00 mM.

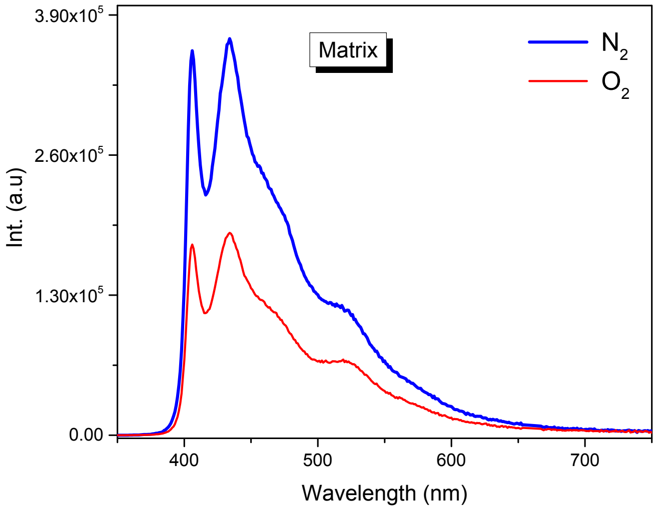

Figure S4. Emission spectrum (λ_{exc} = 330 nm) of a mesoporous solid matrix (SiO_2) under the atmosphere of 100 % N_2 and 100 % O_2.

Table S1**.** Energies of the 10 lowest excited states (singlets-triplets) for monomer and dimer calculated by TD-DFT, both in Dicloromethane (DCM). The highest contributions for each state are shown in terms of molecular orbitals.

State	Transition wavelengths (nm)	Contributions MO (%)
Monomer		
T_1	351 nm	HOMO → L+4 (85%)

		HOMO → L+9 (3%)
T_2	350 nm	H-1 → L+4 (72%) H-2 → L+4 (15%) H-3 → L+4 (6%)
T_3	350 nm	H-2 → L+4 (74%) H-1 → L+4 (15%)
T_4	344 nm	HOMO → LUMO (34%) HOMO → L+1 (29%) HOMO → L+2 (11%)
T_5	343 nm	H-1 → L+2 (43%) H-2 → LUMO (9%) H-2 → L+1 (9%) H-1 → LUMO (7%)
S_1	329 nm	HOMO → LUMO (36%) HOMO → L+1 (35%) HOMO → L+2 (11%)
S_2	328 nm	H-2 → L+1 (29%) H-2 → LUMO (22%) HOMO → L+1 (11%) H-1 → L+3 (11%)
S_3	328 nm	H-1 → L+2 (59%) H-1 → LUMO (16%)
S_4	327 nm	H-2 → L+3 (40%) H-1 → L+3 (15%) H-2 → LUMO (8%)
S_5	321 nm	HOMO → L+4 (92%)

Dímer

T_1	354 nm	HOMO → L+8 (34%) H-2 → L+9 (25%) H-2 → L+8 (11%) HOMO → L+9 (9%)
T_2	354 nm	HOMO → L+9 (32%) H-2 → L+8 (28%) HOMO → L+8 (12%) H-2 → L+9 (10%)
T_3	353 nm	H-1 → L+8 (23%) H-3 → L+8 (19%) H-5 → L+9 (9%)
T_4	352 nm	H-1 → L+9 (27%) H-1 → L+8 (14%) H-5 → L+8 (10%) H-3 → L+8 (10%)
T_5	351 nm	H-5 → L+8 (19%) H-5 → L+9 (16%) H-3 → L+8 (16%) H-3 → L+9 (14%)
S_1	329 nm	HOMO → LUMO (25%) H-1 → LUMO (19%) H-5 → L+2 (7%) HOMO → L+1 (7%)

S_2	329 nm	H-3 → L+4 (32%) H-1 → L+4 (10%) H-2 → L+4 (9%)
S_3	329 nm	H-5 → L+3 (15%) H-1 → L+2 (13%) H-1 → L+3 (12%) H-4 → L+2 (8%)
S_4	328 nm	H-5 → L+2 (13%) H-1 → L+1 (8%) H-3 → L+4 (8%) H-1 → L+3 (7%) H-5 → L+3 (7%)
S_5	328 nm	HOMO → L+1 (26%) H-2 → L+6 (9%) HOMO → L+3 (9%) H-2 → L+7 (8%) H-1 → L+1 (6%)

Table S2**.** Energy of ground singlet and excited triplet states of 1 as a monomer and dimer, respectively.

	ElectronicEnergies (hartree) in CH_2Cl_2	
	Dimer - Triplet	Monomer – Singlet (+ Ghost)
Hartree	-3644,6508	-1822,349901
eV	-99176,036	-49588,685

The energy of the excited triplet state ($E_{excimer}$) was calculated by taking into account the Basis Set Superposition Error (BSSE), by computing the ground (singlet) state energy of the monomer in the presence of ghost atoms belonging to the other monomer (value shown in the table above) and using:

$$E_{excimer} = E_{dimer,triplet} - 2xE_{monomer,ghosts}$$

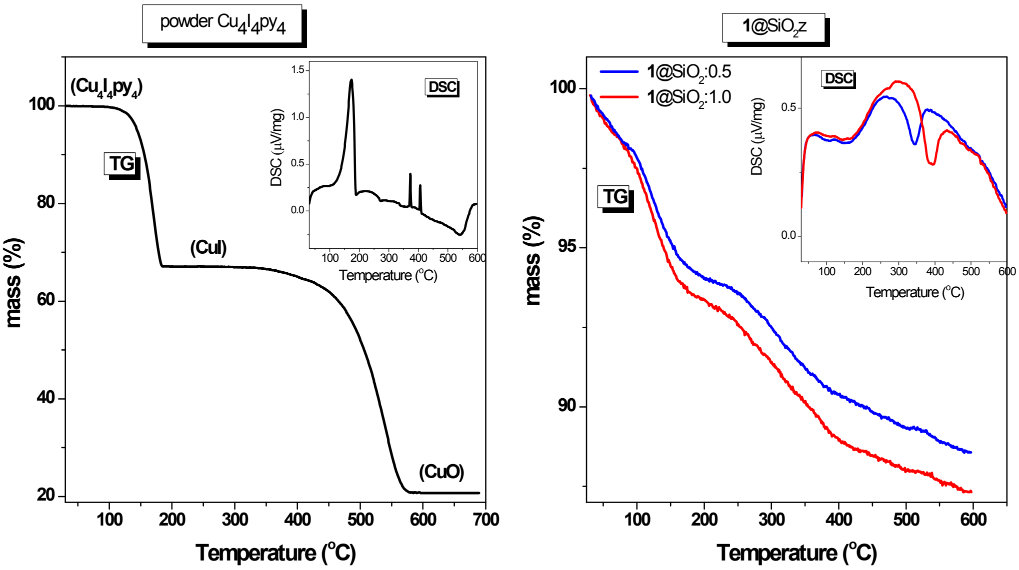

Figure S5. TG and DSC analysis for sample $Cu_4I_4py_4$ powder and loaded in the mesoporous silica matrix (**1**@SiO_2).

According with the TG curve of Figure S5, the gradual increase of temperature of 30 °C to 600 °C decomposes Cu4I4py4 complex in CuI which in turn is decomposed CuO with increasing temperature. The first weight loss (90-185 ° C) is related to decomposition of $Cu_4I_4py_4$ in CuI with a loss of 33% by mass. This mass loss is accompanied by a peak at 172 °C on the DSC curve, the detail in figure S5 (a). The theoretical value calculated for this first mass loss of the complex was 29% which is related to decomposition of pyridine ligands, this value is very close to the experimental value of 33%. The second weight loss (340-580 °C) is related to decomposition of CuO to CuI in the mass loss of 58%. The theoretical value calculated for the second mass loss was 58%, being in excellent agreement with experimental data. The decomposition of CuI with increasing temperature, is also accompanied by two other peaks at 372 ° C and 407 ° C on the DSC curve (the detail in figure S5 (a)).

Figure S5 (b) shows TG curves of the samples 1@SiO_2-0.5 and 1@SiO_2-1.0. In detail figure S5 (b) is also presented the DSC curve of the same samples. Analyzing the TG curves observed that samples of silica loaded with the copper (I) complex have gradual mass loss processes depending on the concentration of loaded $Cu_4I_4py_4$. To the sample 1@SiO_2-0.5, the total mass loss (up to 600 ^{o}C) was 11.5% for 1@SiO_2-1.0 sample loss was 12.7%. According to the experimental results of x-ray fluorescence (XRF) obtained from the embedded SiO_2 sample with $Cu_4I_4py_4$, indicating the approximate concentration of the incorporated complex in the pores of the SiO_2 matrix mass losses of these samples should be 0.3 % and 0.9% for samples 1@SiO_2-0.5 and 1@SiO_2-1.0, respectively. However, we believe that the ionic liquid 1-Butyl-3-methylimidazolium tetrafluoroborate ([Bmim] [PF_6]), used for the formation of pores in the matrix during the sol-gel process has not been completely removed from the pores via soxhlet extraction. The DSC detail in Figure S5 (b) shows two exothermic peaks at 346 ^{o}C and 390 ^{o}C for samples 1@SiO_2-0.5 and 1@SiO_2-1.0, respectively. According to other studies, the decomposition of the cation [Bmim]$^{+}$

occurs between 275-450 °C [1,2]. Thus, the largest contribution to the mass loss of the samples 1@SiO_2-z (z = 0.5, 1.0) would be related to IL traces not completely removed from the pores. However, IL contained in the pores not acted significantly, which could be observed, the photophysical properties of complex hosted in the pores of the matrix.- or that harmed in its characterization.

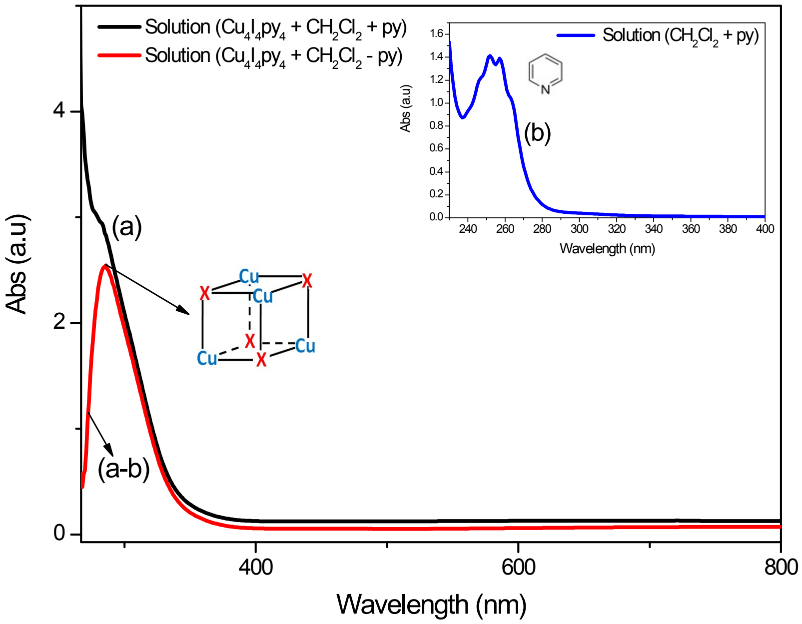

Figure S6. Black curve (a): Absorption spectrum of solution $Cu_4I_4py_4$ 10^{-5}M and pyridine 10^{-6} M in dichloromethane (CH_2Cl_2). Red curve (a-b): Absorption spectrum subtracted pyridine. Inset (b): Absorption spectrum of solution of (CH_2Cl_2 + py).

1. Adela Fernandez, Jose S. Torrecilla, Julian Garcıa, and Francisco Rodriguez, J. Chem. Eng. Data 2007, 52, 1979-1983

2. Holbrey, J. D.; Reichert, W. M.; Swatloski, R. P.; Broker, G. A.; Pitner, W. R.; Seddon, K. R.; Rogers, R. D. Green Chem. 2002, 4, 407-413.